Theoretical Analysis of the Electron Spin Density Distribution of the Flavin Semiquinone Isoalloxazine Ring within Model Protein Environments

José I. García,[†] Milagros Medina,[‡] Javier Sancho,[‡] Pablo J. Alonso,[§] Carlos Gómez-Moreno,[‡] José A. Mayoral,[†] and Jesús I. Martínez*[,§]

Departamento de Química Orgánica, Instituto de Ciencia de Materiales de Aragón, Consejo Superior de Investigaciones Científicas, Universidad de Zaragoza, 50009 Zaragoza, Spain, Departamento de Bioquímica y Biología Molecular y Celular, Facultad de Ciencias, Universidad de Zaragoza, 50009 Zaragoza, Spain, and Departamento de Física de la Materia Condensada, Instituto de Ciencia de Materiales de Aragón, Consejo Superior de Investigaciones Científicas, Universidad de Zaragoza, 50009 Zaragoza, Spain

Received: December 31, 2001

Flavin cofactors are essential for the biological function of many electron-transfer proteins. The electron spin density distribution in the semiquinone (radical) state of the flavin ring has been calculated using the B3LYP hybrid functional in combination with the EPR−II basis set. Both the isolated flavin and the flavin surrounded by small molecules that mimic the environment found in flavoproteins have been analyzed. The validity of the results has been checked by comparison with experimental hyperfine coupling parameters previously reported. The effects of the flavin/protein interaction on the flavin spin density distribution have been discussed. A peculiar behavior of the spin density in some atoms of the flavin ring is found that could be relevant in understanding reaction mechanisms in flavoproteins.

Introduction

Flavoproteins are ubiquitous electron transfer proteins that contain low-potential flavin cofactors (FAD or FMN), either covalently or noncovalently bound. In biological systems, flavoproteins mediate a large variety of redox transformations, including photosynthesis and respiration.[1] Upon association with the protein moiety, the midpoint redox potentials of flavin cofactors are drastically altered, and often, the semireduced state (semiquinone) is significantly stabilized.[2] This provides many flavoproteins with the unique ability to transfer either one or two electrons at a time and, thus, to mediate crucial electron-transfer processes between two-electron donor/acceptors (such as pyridine nucleotides) and one-electron donor/acceptors (i.e., metal-containing centers).[3]

It has been pointed out that the versatility of protein bound flavins must arise from the interaction of the cofactor redox center, the isoalloxazine ring, with the protein polypeptide chain. Protein/flavin interactions have been shown to determine the redox potential of flavoproteins[4,5] and can, therefore, influence their reactivity. Other properties, such as the electron spin density distribution within the isoalloxazine flavin ring system, might also be affected by the interaction with the protein and influence its reactivity as well. Detailed studies of the electron spin density distribution of bound flavins are needed to determine whether it correlates with redox or functional properties of flavoproteins. In this context, higher-resolution EPR-related techniques, such as electron−nuclear double resonance (ENDOR) and electron spin−echo envelope modulation (ESEEM), can be very useful by providing information on the molecular structure and electron spin density distribution of flavoprotein radicals.[6−8] Several flavoprotein semiquinones, neutral and anionic, have been characterized using ENDOR and three-pulse and four-pulse 1D-ESEEM and 2D-ESEEM hyperfine sublevel correlation (HYSCORE) spectroscopies. These studies have led to the assignment of hyperfine couplings to nuclei at six positions in the isoalloxazine semiquinone ring, namely, N(1), N(3), H(5), H(6), CH_3(8), and N(10) (see labeling in Figure 1), and to the determination of the interaction parameters of these atoms with the electron spin, thus providing an experimental measurement of the electron spin density distribution in flavoprotein semiquinones.[8−15] Hyperfine couplings of some other atoms in the ring have also been obtained in non-protein-bound model flavin semiquinones.[6,16,17] In ad-

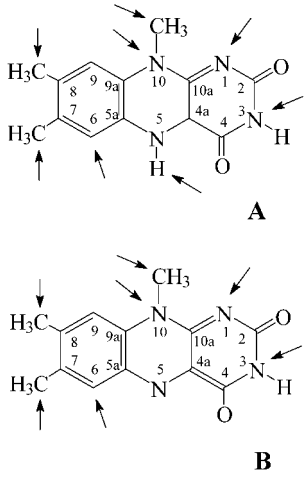

Figure 1. Structures of the neutral (A) and the anionic (B) lumiflavin semiquinone states. Arrows indicate positions of the isoalloxazine ring whose empirical interaction parameters with the unpaired spin have been reported. The numbers for the ring atoms used in the text are also indicated.

* Author for correspondence.
[†] Departamento de Química Orgánica, Universidad de Zaragoza.
[‡] Departamento de Bioquímica y Biología Molecular y Celular, Universidad de Zaragoza.
[§] Departamento de Física de la Materia Condensada, Universidad de Zaragoza.

10.1021/jp014696+ CCC: $22.00
Published on Web 04/17/2002

dition, changes in the electron spin density distribution of the semiquinone radical upon modification of the protein environment have been reported.[9−13,18,19] We notice, however, that the currently available data do not cover all of the nuclei of the isoalloxazine ring and that they derive from the study of just a few flavoproteins. It is thus difficult to draw general conclusions from this reduced data set.

Theoretical calculation of spin densities and hyperfine coupling constants (*A*) have experienced an important development in recent years. Density functional theory, mainly through the use of the hybrid B3LYP functional, in connection with large basis sets has proved to be an excellent theoretical tool in the interpretation of EPR spectra of biological radical molecules. Representative examples are calculations on *p*-benzoquinone and other quinone derivatives,[20] amino acid radicals,[21] and other molecules of biological interest.[22] Some of these studies have taken into account hydrogen bonding and long-range environmental effects on the hyperfine coupling. Theoretical studies have also been applied to the isoalloxazine and the alloxazine rings in order to uncover the electronic bases of their chemical properties. Those studies include calculations of energy levels, electronic densities and other electronic and structural properties of the rings in the different oxidation states by means of both semiempirical and ab initio methods.[23−25] In recent years, some theoretical studies focusing on the influence of the protein environment in shaping the properties of the flavin ring have been reported.[26]

In the present work, we study, by ab initio theoretical calculations using the B3LYP hybrid functional (implemented in Gaussian 98), the spin density distribution in the semiquinone (radical) state for several models of the flavin/protein system. Our most realistic system is a (lumi)flavin molecule surrounded by small organic molecules that mimic hydrogen bonds and π-stacking interactions with the protein. Simpler models containing only specific interactions or a polarizable dielectric continuum are also considered in order to analyze different characteristics of the protein environment that may contribute to the electron spin density distribution of flavoprotein semiquinones. The calculations are validated by comparison with experimentally determined hyperfine couplings.

We have analyzed the π spin density in each atom from a parameter displayed by the Gaussian 98 program, which is proportional to the anisotropic hyperfine coupling. Our data allow for the identifying of the atoms in the flavin ring where most of the spin density is concentrated. The positions that had been previously considered important in flavoprotein reaction mechanisms show high spin density values that are fairly insensitive to changes in the ring environment. This would be an inherent property of the flavin ring that could have been exploited by flavoproteins to preserve the reaction mechanism while evolving toward efficient substrate recognition, binding, and electron transfer in each specific biological system.

Methods

Structural and Experimental Data. For the neutral semiquinone simulation, the three-dimensional conformation of the flavin ring and of its protein environment were taken from oxidized *Anabaena* flavodoxin (Protein Data Bank, PDB, code: 1flv).[27] To simulate the interaction of the N(5) bound proton, only present in the semiquinone state, with the protein environment, data from semireduced *Clostridium beijerinckii* flavodoxin (PDB code: 2fox)[28] were used. The anionic semiquinone conformation was taken from oxidized *Brevibacterium sterolicum* cholesterol oxidase (PDB code: 1cox).[29] Where indicated, some parts of the residues interacting with the isoalloxazine ring in the *Anabaena* flavodoxin structure were included in the calculations. We used the fixed geometry from the X-ray protein structure because it represents a more realistic model for the environment within the protein. For the isolated rings, we also made calculations with the molecule geometry as optimized by Gaussian 98, obtaining very similar results.

ENDOR and one- or two-dimensional ESEEM data for *Anabaena* flavodoxin and *B. Sterolicum* cholesterol oxidase come from previously reported studies.[9,10,14,18] We also make use of previous EPR studies on flavin model systems[6,30] and on other flavoproteins.[6,8,15,19,31]

Theoretical Method. All calculations were carried out with the Gaussian 98 program.[32] The hybrid B3LYP functional,[33,34] as implemented in Gaussian 98, was used throughout this work in spin unrestricted calculations, together with the EPR−II basis set, a combination that has proved to be particularly appropriate for the calculation of spin densities.[35] In particular, it is well-known that the spin contamination of the wave function, expressed as the deviation of the $\langle S^2 \rangle$ expectation value from the exact one (0.75 for a doublet) is considerably less significant in DTF calculations,[36,37] although there is still a controversy about the exact role of spin contamination in Kohn−Sham determinants.[38] In our case, the $\langle S^2 \rangle$ expectation values range from 0.753 to 0.773, before spin projection and annihilation corrections. Long-range environmental effects on the hyperfine constants were estimated using the self-consistent isodensity polarizable continuum model (SCIPCM),[39] as implemented in Gaussian 98. Graphical representations of the spin densities were generated using the GOpenMol program.[40]

Because lumiflavin represents a simple but very accurate model of the redox active moiety of a flavin cofactor (it is identical to FMN except for the sugar−phosphate tail bound to the N(10) position, which is not involved in the redox function), the structure of lumiflavin has been used in the calculations herein described. We have, thus, calculated the spin density of the radical (semiquinone) state of both the neutral and the anionic forms of lumiflavin (Figure 1).

In addition, to simulate the protein environment of a neutral semiquinone, the following systems, inspired in the flavin environment found in flavodoxin, have been calculated:

(a) Lumiflavin embedded in a dielectric continuum. Electric permittivities of either the vacuum (gas-phase molecule), water, or cyclohexane have been used.

(b) Lumiflavin plus hydrogen bonds with relevant residues that interact laterally with the isoalloxazine ring ("in-plane" interactions). Water molecules can substitute for these residues in the calculations with similar results. (Figure 2A)

(c) Lumiflavin with a phenol simulating the "π-stacking" interaction with Tyr94, with an indol simulating the interaction with Trp57, or with both simultaneously (Figure 2B).

(d) A "complete" interaction model including "in-plane" and "π-stacking" interactions.

Data Handling/Analysis. Calculations with Gaussian 98 provide two data sets that can be directly compared to hyperfine parameters obtained from EPR, ENDOR, and ESEEM experiments:

(a) The "isotropic Fermi contact coupling" corresponds to the usual isotropic hyperfine constant, *a*

$$a = (8\pi/3) g_e g_n \beta \beta_n |\psi(R)|^2 \qquad (1)$$

where g_e is the electron gyromagnetic ratio, β is the Bohr magneton, β_n is the nuclear magneton, g_n is the nuclear

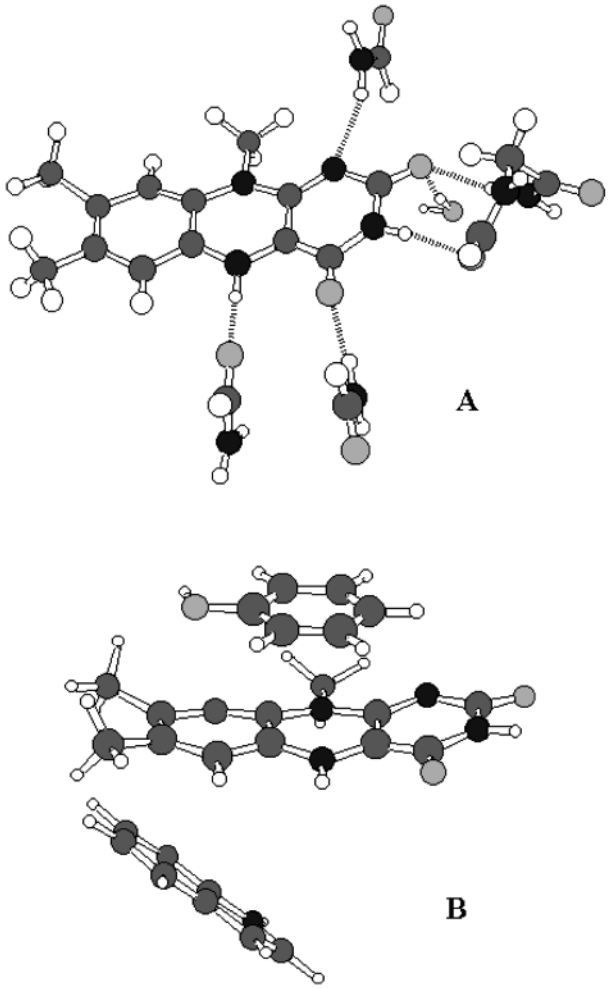

Figure 2. (A) Neutral lumiflavin semiquinone surrounded by the "in-plane" interactions considered in the calculations. (B) Neutral lumiflavin semiquinone with a phenol and an indol simulating Tyr94 and Trp57 "π-stacking" interactions of *Anabaena* flavodoxin.

gyromagnetic ratio of the corresponding nucleus, and $|\psi(R)|^2$ is the spin density at the nucleus.

(b) The "spin dipole coupling", hereafter $\langle r^{-3}\rangle_{ij}$ tensors, that correspond to the anisotropic (traceless) part of the hyperfine tensors T_{ij}[20]

$$T_{ij} = g_e g_n \beta \beta_n \langle r^{-3}\rangle_{ij} \quad (2)$$

These data are displayed by the program when calculating the "spin-only" contribution. Gaussian 98 provides principal values and directions for this anisotropic contribution. Thus, the hyperfine tensor principal values can readily be obtained

$$A_{ii} = a + T_{ii}, \quad i = x, y, z \quad (3)$$

We will also make use of the "axial" (T) hyperfine coupling constant:[14]

$$T = T_{zz}/2 \quad (4)$$

Moreover, Gaussian can be also used to obtain the "electric field gradient" q_{ij} tensors that give the traceless nuclear quadrupolar P_{ij} tensors whose principal values are

$$P_{ii} = (q_{ii} Q e^2)/2I(2I-1), \quad i = x, y, z \quad (5)$$

with Q being the electric quadrupolar moment, I being the nuclear spin of the nucleus, and e being the electron charge. K and η parameters can be defined as[14]

$$K = |P_{zz}|/2$$

$$\eta = (|P_{yy}| - |P_{xx}|)/|P_{zz}| \quad (6)$$

with $|P_{xx}| < |P_{yy}| < |P_{zz}|$.

TABLE 1: Hyperfine and Quadrupolar Parameters for Neutral Flavoprotein Semiquinone (Comparison between Theoretical Calculations and Experimental Data)[a]

	calculated data				experimental data			
atom	a (MHz)	T (MHz)	K (MHz)	η	a (MHz)	T (MHz)	K (MHz)	η
H(5)	−21.4	11.0			−18.8	9.0		
H(6)	−6.4	2.1			−5.7	n.d.[b,c]		
H(met8)	9.1	0.6			8.4	0.5		
H(met10)	9.8	1.0			12.5[d]	1.15[d]		
N(1)	0.1	0.3	0.7	0.8	0.8[e]	n.d.[b]	0.8[e,f]	0.5[e,f]
N(3)	−1.0	0.3	0.8	0.2	1.3[e]	n.d.[b]	0.7−0.9[e]	n.d.[b]
N(5)	13.6	14.6	0.7	0.3	22.1[g]			
N(10)	7.6	7.6	0.8	0.2	11.7	9.0	1.3[h]	

[a] Unless otherwise stated, the experimental data correspond to those reported for *Anabaena* flavodoxin semiquinone obtained by ENDOR and HYSCORE spectroscopies.[14,18] [b] Not determined. [c] Considered being highly anisotropic. [d] Data obtained from flavodoxin reconstituted with lumiflavin. [e] Assignment of the experimental parameters between positions N(1) and N(3) is ambiguous. [f] Estimated from data obtained for cholesterol oxidase. [g] Data reported for model neutral flavin radicals.[6] [h] Approximated value.

Results and Discussion

Calculated versus Experimental Hyperfine Coupling Constants. Theoretical values for the hyperfine interaction parameters of all of the nuclei of the flavin ring with the unpaired spin have been obtained for the neutral and the anionic lumiflavin semiquinones using the hybrid B3LYP functional, which has been shown to provide good results in other radical molecules.[20] To verify the reliability of the method in our particular case, the predicted interaction parameters have been compared with those experimentally obtained. Hyperfine coupling constants for the interaction with the spin semiquinone radical have been reported for the N(1), N(3), H(5), H(6), H in CH_3(8), N(10), and H in CH_3(10) atoms in several flavoproteins, using ENDOR and ESEEM spectroscopies.[6,8−14,18] The experimentally determined interaction parameters reported at those positions for the flavodoxin neutral semiquinone are compared in Table 1 with those obtained in our theoretical calculations for a neutral lumiflavin radical with both "in-plane" and "π-stacking" interactions.

The parameters obtained from theoretical calculations of the anionic lumiflavin radical have been compared with those experimentally reported for the anionic cholesterol oxidase semiquinone in Table 2. In this case, the bare free anionic radical ring was analyzed, because calculations including external interactions did not converge.

Let us review the results of these comparisons for each atom. ESEEM and HYSCORE spectra of flavoprotein semiquinones display peaks corresponding to weak interacting nitrogens that were attributed to N(1) and N(3) in the isoalloxazine ring.[11,12,14] However, only the module of a and partial information about quadrupolar interaction were obtained, and the assignment of each set of parameters to a particular position, N(1) and N(3), was not possible. The data indicated very weak coupling constants for both nuclei and values for the quadrupolar term typical of pyrimidine rings. As shown in Tables 1 and 2, all of

TABLE 2: Hyperfine and Quadrupolar Parameters for Anionic Flavoprotein Semiquinone (Comparison between Theoretical Calculations and Experimental Data)[a]

	calculated data				experimental data			
atom	*a* (MHz)	*T* (MHz)	*K* (MHz)	η	*a* (MHz)	*T* (MHz)	*K* (MHz)	η
H(6)	−11.3	2.7			−9.0	n.d.[b,c]		
H(met8)	13.9	0.6			10.9	0.6		
N(1)	0.7	1.1	0.7	0.8	0.7[d]	n.d.[b]	0.7−0.9[d]	n.d.[b]
N(3)	−1.3	0.1	0.8	0.2	1.9[d]	n.d.[b]	0.8[d]	0.5[d]
N(5)	16.0	17.4	0.7	0.3	20.4[e]			
N(10)	8.2	5.2	0.8	0.2	11.7	9.0	1.3[f]	n.d.[b]

[a] Unless otherwise stated, the experimental data correspond to those reported for *Brevibacterium Sterolicum* cholesterol oxidase semiquinone obtained by ENDOR and HYSCORE spectroscopies.[9,14] [b] Not determined. [c] Considered being highly anisotropic. [d] Assignment of the experimental parameters between positions N(1) and N(3) is ambiguous. [e] Data reported for model anionic flavin radicals.[8] [f] Estimated from flavodoxin data.

these facts are well reflected in the theoretical calculations: the values obtained for the isotropic hyperfine coupling constants for both nuclei are between 0 and 2 MHz (isotropic coupling in the rest of the calculated neutral flavin semiquinone environments, not shown, are between 0 and 3.5 MHz), and the calculated quadrupolar interaction parameters are fully compatible with the experimental ones. Unfortunately, our calculations do not solve the assignment problem. Although the theoretical data of *a* reported in Tables 1 and 2 might indicate that N(1) should be the nucleus exhibiting a smaller value of *a*, and the values of N(1) and N(3) are still too close to one another and vary considerably from one calculation to another (see analysis of Table 3 below).

The hyperfine interaction of N(5) has not been experimentally detected in flavoproteins. However, EPR and ENDOR signals coming from this interaction in liquid solutions of model flavins have been reported, indicating that N(5) must be the nucleus with the strongest hyperfine interaction in the ring.[6,8] Our theoretical calculations also indicate a very strong hyperfine coupling for this nitrogen (Tables 1 and 2). For both neutral and anionic semiquinones, the reported experimental *a* values are higher than the calculated ones. Nevertheless, as pointed out in ref 6, it has to be noted that the tumbling of flavin model complexes in water at room temperature is not fast enough to average completely the anisotropic hyperfine contribution, which could introduce an inaccuracy in the experimentally determined constant. Furthermore, our calculations suggest that the anisotropy of the interaction had been underestimated.[6,17]

HYSCORE spectra of neutral flavoprotein semiquinones display a hydrogen correlation ridge that was assigned to the H(5) nucleus. From this ridge, and assuming a nearly axial hyperfine interaction, values of −18.8 and 9.0 MHz have been determined for the isotropic (*a*) and axial (*T*) hyperfine coupling constants, respectively.[14] Slightly larger values (21−23 MHz) for the isotropic hyperfine coupling constant have also been experimentally reported for model compounds.[6] The theoretical value obtained for *a* of H(5) is very similar to the experimental ones, especially to those of model compounds (Table 1). Besides, our calculated *T* value for H(5) is compatible with the experimental one. It is noteworthy that the calculations indicate an important orthorhombic component in the interaction. If this were the case, the ridge observed in the HYSCORE spectra could just constitute a part of the complete feature.

The interaction of the flavin radical with H(6) has been detected in the ENDOR spectra of both, flavoproteins and model flavin compounds.[6,8] The theoretically calculated values of *a* for both neutral and anionic semiquinones correspond quite well to the experimental ones (Tables 1 and 2). Previous analyses assumed that the H(6) hyperfine interaction should be largely anisotropic,[8−10,13] but the theoretical calculations reported here do not support that assumption and clearly indicate a small anisotropy for the H(6) hyperfine coupling. The anisotropic part of the H(6) interaction has not been directly measured. Generally, the ENDOR spectra only show a single H(6) feature that was considered as a part of the complete, not observable, orthorhombic signal. However, such a feature could also be interpreted on the basis of an interaction with a relatively small anisotropy.

The hydrogen hyperfine interaction of the semiquinone radical with the rapidly rotating methyl group CH_3(8) has been well characterized from ENDOR measurements.[8] There is a difficulty in comparing calculated and measured parameters for rotating

TABLE 3: Z Eigenvalue of the $\langle r^{-3}\rangle_{ij}$ Tensor (Atomic Units × 100) of Some Atoms of Anionic and Neutral Lumiflavin Semiquinones

	anionic	neutral semiquinone							
atom	gas phase[a]	gas phase[a]	ϵ_{H_2O}[b]	$\epsilon_{cyclohex}$[c]	in plane[d]	phenol[e]	indol[f]	π stack[g]	all[h]
N(1)	5.7	14.2	1.6	4.9	1.7	12.9	12.8	11.9	1.5
C(2)[i]	1.2	−1.5	−0.4	−0.7	−0.9	−2.2	−2.2	−2.1	−0.9
O(2)	15.1	20.5	11.3	17.6	12.8	26.6	26.1	25.4	12.5
N(3)[i]	−0.7	1.8	1.7	2.4	1.8	1.6	1.6	1.6	1.8
C(4)[i]	4.6	−1.8	3.8	3.0	3.4	−1.8	−1.8	−1.8	3.8
O(4)	27.0	40.0	35.1	36.8	32.2	44.0	44.2	43.3	32.6
C(4a)	16.7	46.4	26.5	35.3	29.5	40.7	40.1	39.7	29.0
N(5)	90.3	72.4	75.7	71.7	77.4	66.2	67.7	67.0	73.9
C(5a)[i]	−10.2	−4.0	4.2	−1.8	−2.1	−3.9	−3.6	−3.5	−1.6
C(6)	17.0	6.3	6.7	8.3	9.8	9.6	9.2	9.5	9.6
C(7)	−7.3	−1.8	1.5	−0.6	−1.0	−2.1	−1.5	−1.7	−0.7
C(8)	21.3	9.9	19.9	17.1	17.8	15.1	15.3	15.5	17.8
C(9)	−4.8	−3.4	−7.5	−6.4	−6.0	−4.6	−5.2	−4.8	−5.4
C(9a)	13.3	8.2	12.5	9.6	9.7	8.0	8.3	8.3	9.6
N(10)	26.9	28.4	39.7	37.5	41.2	29.2	30.9	29.8	39.4
C(10a)[i]	5.1	−2.7	−2.5	−1.5	1.0	−3.2	−3.3	−3.0	−0.9

[a] Isolated molecule in a vacuum. [b] Isolated molecule embedded in a medium with the dielectric permittivity of water. [c] Isolated molecule embedded in a medium with the dielectric permittivity of cyclohexane. [d] Molecule in a vacuum with the lateral interacting residues, as shown in Figure 2A. [e] Molecule in a vacuum with a phenol simulating the Tyr94 π stacking in the protein. [f] Molecule in a vacuum with an indol simulating the Trp57 π stacking in the protein. [g] Molecule in a vacuum with both a phenol and an indol simulating the complete π stacking in the protein, as shown in Figure 2B. [h] Molecule in a complete interaction model including "in-plane" and π-stacking interactions. [i] The $\langle r^{-3}\rangle_{ij}$ tensor of this atom has a large orthorhombicity and/or the principal direction of its largest eigenvalue deviates noticeably from *Z* axis.

methyl groups because the calculations only provide the interaction of the three static hydrogen nuclei in a given orientation. Values for *a* and *T* have been estimated by averaging the three hyperfine tensors obtained in the calculations. This would correspond to a jumping process between the three hydrogen positions rather than to a continuous tumbling, but it gives an acceptable estimation for the actual interaction parameters, which correlates well with the experimentally reported values (Tables 1 and 2).

Although flavoproteins do not contain lumiflavin as a prosthetic group, experimental data for the interaction parameters of the protons in a methyl group $CH_3(10)$ have been reported from ENDOR studies on semiquinone model compounds and also from the neutral semiquinone of a lumiflavin reconstituted flavodoxin (LM-Fld).[6,18] These reported values can thus be consider for comparison with our theoretical data that, as in the case of $CH_3(8)$, have been obtained by averaging the three static hydrogen hyperfine tensors. The calculated isotropic and axial parameters are similar to the experimental ones reported for LM-Fld neutral semiquinone (Table 1).

A correlation ridge that was assigned to the hyperfine interaction of the spin radical with the N(10) nucleus of the flavin was detected in the HYSCORE spectra of several flavoprotein semiquinones.[14] From the analysis of this signal, the isotropic and axial parameters were obtained, as well as an estimation of the quadrupolar interaction constant, *K*. As shown in Tables 1 and 2, the theoretically calculated hyperfine parameters slightly shift from the experimental ones. It should be noticed, however, that the empirical data correspond to FMN or FAD semiquinones, which differ from lumiflavin in bearing substituents at the studied position 10.

Finally, it should be remembered that, besides the lack of a H(5) interaction signal, additional empirical differences in the hyperfine coupling of anionic and neutral semiquinones had been reported:[6,8] the *a* values for couplings of H(6) and H in $CH_3(8)$ to the spin radical are larger in module for the anionic semiquinones, whereas the *a* value for H in $CH_3(10)$ is lower. These differences are clearly predicted by our theoretical calculations (Tables 1 and 2).

In summary, we find a good agreement between experimental data and calculations using the hybrid B3LYP functional with lumiflavin semiquinone, which suggests that our calculations provide a representative model of the spin distribution within the flavin ring.

Calculation of the Electron Spin Density Distribution within the Flavin Ring Semiquinone. Given that the knowledge of the spin distribution in flavin semiquinone has been considered of mechanistic importance for suggesting electron transfer,[8] attempts have been made to get a map, as complete as possible, of the spin distribution in the flavin ring. Previous studies combining data from EPR and ENDOR experiments with semiempirical calculations,[8,17,24] as well as ab initio theoretical calculations[25] have been reported. As flavin ring radicals are expected to be planar π radicals, spin populations in the SOMO, which is a π orbital, have to be determined. Until the past decade, only a few EPR or ENDOR data on the hyperfine parameters of some hydrogen and nitrogen nuclei in the flavin were available. Therefore, an indirect approach was used in order to obtain information about the spin densities in the π (p_z) orbitals with this incomplete information. It has been demonstrated that spin densities in the nuclei of a planar π radical are related with spin polarization in their corresponding bound hydrogens, so this relation can be applied:

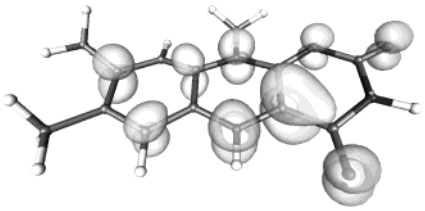

Figure 3. UB3LYP/EPR−II spin density plot for the neutral flavin radical.

$$a^{\mathrm{H}} = Q_{\mathrm{H}-x}\rho_x \tag{7}$$

where ρ_x is the spin density in the π orbital for the *x* atom in the ring, a^{H} is the isotropic hyperfine coupling constant for the hydrogen bound to *x*, and $Q_{\mathrm{H}-x}$ is a semiempirical "spin polarization parameter".[17] Simpler, less theoretically supported expressions, such as

$$a^x = Q_x\rho_x \tag{8}$$

which relate spin density ρ with the *a* value of the same nucleus *x*, have also been used.[8,41] In any case, these methods are approximations that cannot account for the spin densities at every atom of the ring.

Our calculations provide a detailed information about spin densities at every atom (Figure 3). This makes unnecessary the use of expressions such as (7) or (8). Tables of calculated isotropic hyperfine parameters, like those reported in ref 25, are useful for comparison with experimental values but are not the most appropriate to face the problem of the spin densities.

When studying other planar π-radical systems, O'Malley[20] has pointed out that the anisotropic coupling tensor $\langle r^{-3}\rangle_{ij}$ is a direct measure of the spin density in the atom. When the spin is localized in a pure p_z orbital, the contact term $|\psi(R)|^2$ is due to polarization of the s orbitals, and it is small. Besides, the anisotropic tensor $\langle r^{-3}\rangle_{ij}$ must be nearly axial, being *Z* the principal axis. The tensor can deviate from this behavior when the spin density in the atom is small and the densities in neighboring atoms affect the values of $\langle r^{-3}\rangle_{ij}$, or when there is an important admixture of σ orbitals with the π one. If $\langle r^{-3}\rangle_{ij}$ is axial (given that it is traceless) a constant, namely its principal value in the Z direction $\langle r^{-3}\rangle_{zz}$, is enough to characterize the tensor:

$$\langle r^{-3}\rangle_{xx} = \langle r^{-3}\rangle_{yy}, \quad \langle r^{-3}\rangle_{xx} + \langle r^{-3}\rangle_{yy} + \langle r^{-3}\rangle_{zz} = 0$$

$$\langle r^{-3}\rangle_{zz} = -2\langle r^{-3}\rangle_{xx} \tag{9}$$

and it is proportional to the spin density in the atom.

We have taken all of these considerations into account for our analysis. First, we have tested the orthorhombicity and orientation of the $\langle r^{-3}\rangle_{ij}$ principal axes in each atom of the ring. Positions C(2), N(3), C(4), and C(6a) show a noticeable orthorhombicity and/or principal axes that depart from *Z* by more than 15°. They correspond to positions where the eigenvalue of $\langle r^{-3}\rangle_{ij}$ with the highest module is very small. All of the other atoms show the expected behavior for a π spin density. This is also true for O atoms bound to C(2) and C(4), whereas methyl C atoms bound to C(7), C(8), and C(10) are not involved in the π radical.

The value of $\langle r^{-3}\rangle_{zz}$ obtained from our calculations is then used to characterize the π spin density in neutral and anionic lumiflavin semiquinones. It is worth noting that, in these types of systems, the anisotropic part of the experimentally determined

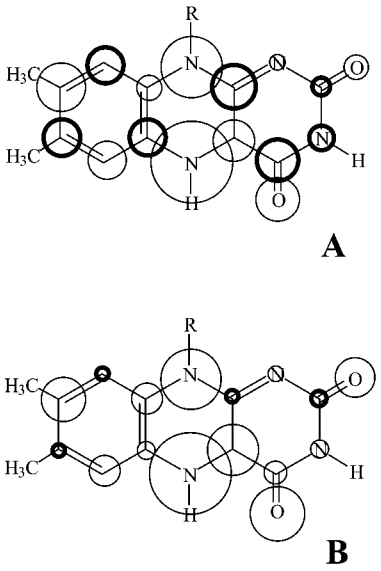

Figure 4. Representation of the calculated distribution of spin density in flavin neutral semiquinones by circles on the ring atoms: (A) using the isotropic spin density at the nucleus $|\psi(R)|^2$ and (B) using the Z eigenvalue of $\langle r^{-3}\rangle_{ij}$ tensor. Bold circles correspond to negative values.

hyperfine tensor is also a more valuable data for analyzing spin densities, and when available, it should be preferred to the isotropic one. To illustrate this fact, Figure 4 shows a representation of the spin densities by mean of circles on the atoms of the ring, using $|\psi(R)|^2$ or the Z eigenvalue of the $\langle r^{-3}\rangle_{ij}$ tensor. It is evident that, in the first case, the spin densities in atoms where the π contribution is weaker tend to be overestimated. Other quantitative differences also occur. Noticeably, although Figure 4B shows important similarities with that of Edmondson,[8] our calculations reveal important spin densities in the oxygen atoms that were not considered before. The figure shows also the sign of $\langle r^{-3}\rangle_{zz}$ for the flavin ring atoms, which alternates from one to the next (the small contributions of C(4) and C(5a) can be ignored because they change their sign from a calculation to another), except for the couples C(4a)−N(5) and C(9a)−N(10), where both signs are positive.

Calculated values of $\langle r^{-3}\rangle_{zz}$ (Table 3) clearly predict that the anionic flavin semiquinone has a larger spin density on the benzene ring and on the N(5) position than the neutral one. On the other hand, less spin density is predicted on the N(1), O(2), C(4a), and O(4) atoms of the anionic semiquinone than in equivalent ones of the neutral. These data are fully consistent with those experimentally obtained in flavin model systems.[8,16,17] In contrast, our calculations indicate that the spin density is larger on the C(4a) position of the neutral semiquinone than in the anionic one, which is not in agreement with previously reported data.[8]

Influence of the Protein Environment in the Electron Spin Density Distribution of the Neutral Flavin Radical. For the neutral lumiflavin semiquinone, calculations have also been carried out to model the effect that the protein environment exerts in the spin density distribution. We have considered the influence of the electric permittivity of the medium and, inspired in the FMN interactions in flavodoxin, have simulated "in-plane" and "π-stacking" protein interactions, both independent and simultaneously. The values obtained for $\langle r^{-3}\rangle_{zz}$ are reported in Table 3 and can be summarized as follows.

Positions indicated with a superscript *i*, C(2), N(3), C(4), C(5a), and C(10a), show small values and important variations (relative to their total value). As we have explained above, data for these atoms are not very informative because the principal direction does not follow the Z axis, and the values here collected are the ones for the principal direction closest to Z. Even the sign of the eigenvalues fluctuates. This is also observed with the values obtained for C(7), that are very small although in this case they always have a $\langle r^{-3}\rangle_{ij}$ tensor axial with respect to Z. These are all positions with small spin densities and will not be considered relevant in our discussion.

The introduction of a continuum electric permittivity, either that of water or cyclohexane, produces almost the same $\langle r^{-3}\rangle_{zz}$ values as including "in-plane" interactions for the different atoms of the flavin ring. This can be understood because the hydrogen bonds introduced by the "in-plane" interactions produce a polarization effect similar to that of the change in the permittivity. In both cases the absolute value of the Z eingenvalue tends to decrease in the "pyrimidine" atoms of the isoalloxazine ring [N(1), O(2), O(4), and C(4a)], whereas it increases in those of the "benzenoid" ring [C(6), C(8), C(9), and C(9a)] and in N(10). The largest relative changes are observed for N(1), O(2), C(8), and C(9) atoms.

The data reported in Table 3 indicate that changes induced in the Z eigenvalue by "π-stacking" interactions, either considering an indol (tryptophan), a phenol (tyrosine), or both simultaneously, produce only moderate effects for most of the flavin atoms. The largest changes (relative to the total value in the atom) take place on the two oxygen atoms [O(2) and O(4)] and in positions C(6), C(8), and C(9) in the "benzenoid" ring. A relatively moderate decrease in the C(4a)−N(5) zone is also noticeable.

Finally, when a full model having into account the "in-plane" and "π-stacking" interactions observed in flavodoxin was calculated, the Z eigenvalues nearly match those obtained by having into account only the "in-plane" interactions. This clearly indicates that "in-plane" interactions exert most of the spin density modulation, whereas "π-stacking" interactions might only have some effect in the spin densities of the nitrogen atoms in the "pyrazine" ring [N(5) and N(10)] or on those positions where they produce effects comparable to those of the "in-plane" interactions [C(4a), C(6), C(8), and C(9)]. These results are consistent with previous experimental studies on several flavodoxin mutants,[18] where it was demonstrated that only subtle differences in H(5), H(6), and H in CH_3(8) isotropic hyperfine coupling constants appeared by changing or removing the "π-stacking" residues.

Although we have analyzed the effect of the protein environment using that of a given flavodoxin, our discussion can also apply for many flavoproteins. It has been pointed out that H-bonds involving the "pyrimidine" atoms [N(1), O(2), N(3), O(4), and N(5)] are present in most flavoproteins, and π-stacking interactions are very frequent as well.[26] Our calculations provide a general guide for understanding the effects of flavin−apoprotein interactions on the flavin radical spin density distribution.

Among the atoms with the largest spin densities, N(5) displays quite a peculiar behavior. The protein environment, especially the "in-plane" interactions, exerts a considerable influence on most of the atoms exhibiting high spin density: C(4a), N(10), O(4), or O(2). In all these positions, interaction with the apoprotein causes relative changes larger than 25%. In contrast, the spin density of N(5) remains rather stable, although it holds the largest density. This seems relevant, because position N(5) has been considered as one of the electron transfer sites from/to the flavin ring in many flavoproteins. This suggests that it could have been advantageous for proteins to use a redox

cofactor which preserves a high, stable spin density in the key atom that would be involved in the redox transfer process. This may have contributed to avoid unwanted, somewhat random redistributions of the cofactor spin density as side effects upon evolution of the protein binding site. On the other hand, the flavin radical does not significantly delocalize spin density into the protein, as shown by the fact that the sum of all of the $\langle r^{-3}\rangle_{zz}$ eigenvalues in the ring is nearly constant for every calculated system. This indicates that the local changes observed in the spin densities are caused by a redistribution of the π density within the flavin ring.

It has already been noted[8] that spin density in the "benzenoid" part of the ring is small, although in many cases this is the one closest to the substrate. In this part of the flavin ring, the C(8) position has usually been considered important for some reaction mechanisms. Our calculations could also support this idea. Except for the isolated ("gas phase") neutral flavin radical, in all of the "interacting" calculated flavins, C(8) shows the largest and most stable spin density among the "benzenoid" part atoms. Therefore, this atom could play for the "benzenoid" ring a similar role to that of N(5) for the complete flavin ring.

In conclusion, we have demonstrated that calculation of the spin density in flavin semiquinone using the hybrid B3LYP functional in combination with the EPR−II basis set provides very realistic results for both the isolated molecule and a system that models the flavin−apoprotein interaction. Comparison of the spin density in the atoms in the flavin ring for the different flavin−protein interactions analyzed shows that some atoms of the flavin preserve a stable high spin density. This appears to be a property of the flavin radical that could influence its electron-transfer mechanisms and could have been advantageous for the evolution of flavoproteins.

Acknowledgment. This work was supported by Grants PB97-1027 from DGES and P15/97 from CONSI+D (DGA) to J.S., by Grant P15/98 from CONSI+D (DGA) to P.J.A., by Grant UZ97-CIE−09 from the Universidad de Zaragoza to J.I.M., by Grant P006/2000 from CONSI+D (DGA) to M.M., and by Grant MAT99-1176 from CICYT to J.A.M. and J.I.G.

References and Notes

(1) (a) *Flavins and Flavoproteins*; Edmondson, D. E., McCormick, D. B., Eds.; Walter de Gruyter: Berlin, 1987. (b) *Flavins and Flavoproteins*; Yagi, K., Ed.; Walter de Gruyter: Berlin, 1993. (c) *Flavins and Flavoproteins*; Ghisla, S., Kröneck, P., Macheroux, P., Sund, H., Eds.; Agency for Scientific Publ.: Berlin, 1999.

(2) Mayhew, S. G.; Tollin, G. In *Chemistry and Biochemistry of Flavoenzymes*; Müller, F., Ed.; CRC Press: Boca Raton, FL, 1992; Vol. III, pp 389−426.

(3) *Chemistry and Biochemistry of Flavoenzymes*; Müller, F., Ed.; CRC Press: Boca Raton, FL, 1992; Vol. III.

(4) Zhou, Z. M.; Swenson, R. P. *Biochemistry* **1996**, *35*, 15980.

(5) Lostao, A.; Gómez-Moreno, C.; Mayhew, S. G.; Sancho, J. *Biochemistry* **1997**, *36*, 14334.

(6) Kurreck, H.; Bock, M.; Bretz, N.; Elsner, M.; Kraus, H.; Lubitz, W.; Müller, F.; Geissler, J.; Kroneck, P. M. H. *J. Am. Chem. Soc.* **1984**, *106*, 737.

(7) Kurreck, H.; Kirste, B.; Lubitz, W. In *Electron Nuclear Double Resonance Spectroscopy of Radicals in Solution*; Marchand, A. P., Ed.; VCH: Weinheim, Germany, 1988; pp 279−331.

(8) Edmondson, D. E. *Biochem. Soc. Trans.* **1985**, *13*, 593.

(9) Medina, M.; Vrielink, A.; Cammack, R. *Eur. J. Biochem.* **1994**, *222*, 941.

(10) Medina, M.; Gómez-Moreno, C.; Cammack, R. *Eur. J. Biochem.* **1995**, *227*, 529.

(11) Medina, M.; Cammack, R. *J. Chem. Soc., Perkin Trans. 2* **1996**, 633.

(12) Medina, M.; Vrielink, A.; Cammack, R. *FEBS Lett.* **1997**, *400*, 247.

(13) Çinkaya, I.; Buckel, W.; Medina, M.; Gómez-Moreno, C.; Cammack, R. *Biol. Chem.* **1997**, *378*, 843.

(14) Martínez, J. I.; Alonso, P. J.; Gómez-Moreno, C.; Medina, M. *Biochemistry* **1997**, *36*, 15526.

(15) Hung, S.-C.; Grant, C. V.; Peloquin, J. M.; Waldeck, A. R.; Brit, R. D.; Chan, S. I. *J. Biol. Inorg. Chem.* **2000**, *5*, 593.

(16) Ehrenberg, A.; Müller, F.; Hemmerich, P. *Eur. J. Biochem.* **1967**, *2*, 286.

(17) Müller, F.; Hemmerich, P.; Ehrenberg, A.; Palmer, G.; Massey, V. *Eur. J. Biochem.* **1970**, *14*, 185.

(18) Medina, M.; Lostao, A.; Sancho, J.; Gómez-Moreno, C.; Cammack, R.; Alonso, P. J.; Martínez, J. I. *Biophys. J.* **1999**, *77*, 1712.

(19) Macheroux, P.; Petersen, J.; Bornemann, S.; Lowe, D. J.; Thornley, R. N. F. *Biochemistry* **1996**, *35*, 5: 1643.

(20) (a) O'Malley, P. J. *J. Phys. Chem. A* **1997**, *101*, 6334. (b) O'Malley, P. J. *J. Phys. Chem. A* **1998**, *102*, 248.

(21) (a) O'Malley, P. J. *J. Am. Chem. Soc.* **1998**, *120*, 11732. (b) Rega, N.; Cossi, M.; Barone, V. *J. Am. Chem. Soc.* **1998**, *120*, 5723. (c) Ivancich, A.; Mattioli, T. A.; Un, S. *J. Am. Chem. Soc.* **1999**, *121*, 5743.

(22) (a) Wetmore, S. D.; Boyd, R. J.; Eriksson, L. A. *J. Phys. Chem. B* **1998**, *102*, 9332. (b) Lahorte, P.; Deproft, F.; Callens, F.; Geerlings, P.; Mondelaers, W. *J. Phys. Chem. A* **1999**, *103*, 11130. (c) O'Malley, P. J. *J. Comput. Chem.* **1999**, *20*, 1292.

(23) (a) Szymusiak, H.; Konarski, J.; Koziol, J. *J. Chem. Soc., Perkin Trans. 2* **1990**, 229. (b) Zheng, Y.-J.; Ornstein, R. L. *J. Am. Chem. Soc.* **1996**, *118*, 9402. (c) Nakai, S.; Yoneda, F.; Yamabe, T. *Theor. Chem. Acc.* **1999**, *103*, 109.

(24) Song, P.-S. *Ann. N. Y. Acad. Sci.* **1969**, *158*, 410.

(25) Zielinski, R.; Szymusiak, H. In *Flavins and Flavoproteins*; Ghisla, S., Kröneck, P., Macheroux, P., Sund, H., Eds.; Agency for Scientific Publ.: Berlin, 1999; pp 59−62.

(26) (a) Rotello, V. In *Flavins and Flavoproteins*; Ghisla, S., Kröneck, P., Macheroux, P., Sund, H., Eds.; Agency for Scientific Publ.: Berlin, 1999; pp 17−22. (b) Watanabe, Y. In *Flavins and Flavoproteins*; Ghisla, S., Kröneck, P., Macheroux, P., Sund, H., Eds.; Agency for Scientific Publ.: Berlin, 1999; pp 53−58.

(27) Rao, S. T.; Shaffie, F.; Yu, C.; Satyshur, K. A.; Stockman, B. J.; Markley, J. L.; Sundaralingan, M. *Protein Sci.* **1992**, *1*, 1413.

(28) Smith, W. W.; Burnett, R. M.; Darling, G. D.; Ludwig, M. L. *J. Mol. Biol.* **1977**, *117*, 195.

(29) Li, J.; Vrieling, A.; Brick, P.; Blow, D. M. *Biochemistry* **1993**, *32*, 11507.

(30) Eriksson, L. E. G.; Hyde, J. S.; Ehrenberg, A. *Biochim. Biophys. Acta* **1969**, *192*, 211.

(31) Ehrenberg, A.; Eriksson, L. E. G.; Hyde, J. S. *Biochim. Biophys. Acta* **1968**, *167*, 482.

(32) Frisch, M. J.; Trucks, G. W.; Schlegel, H. B.; Scuseria, G. E.; Robb, M. A.; Cheeseman, J. R.; Zakrzewski, V. G.; Montgomery, J. A., Jr.; Stratmann, R. E.; Burant, J. C.; Dapprich, S.; Millam, J. M.; Daniels, A. D.; Kudin, K. N.; Strain, M. C.; Farkas, O.; Tomasi, J.; Barone, V.; Cossi, M.; Cammi, R.; Mennucci, B.; Pomelli, C.; Adamo, C.; Clifford, S.; Ochterski, J.; Petersson, G. A.; Ayala, P. Y.; Cui, Q.; Morokuma, K.; Malick, D. K.; Rabuck, A. D.; Raghavachari, K.; Foresman, J. B.; Cioslowski, J.; Ortiz, J. V.; Stefanov, B. B.; Liu, G.; Liashenko, A.; Piskorz, P.; Komaromi, I.; Gomperts, R.; Martin, R. L.; Fox, D. J.; Keith, T.; Al-Laham, M. A.; Peng, C. Y.; Nanayakkara, A.; Gonzalez, C.; Challacombe, M.; Gill, P. M. W.; Johnson, B. G.; Chen, W.; Wong, M. W.; Andres, J. L.; Head-Gordon, M.; Replogle, E. S.; Pople, J. A. *Gaussian 98*, revision A.7; Gaussian, Inc.: Pittsburgh, PA, 1998.

(33) Lee, C.; Yang, W.; Parr, R. *Phys. Rev. B* **1988**, *37*, 785.

(34) Becke, A. D. *J. Chem. Phys.* **1993**, *98*, 5648.

(35) Barone, V. In *Recent Advances in Density Functional Methods*; Chong, D. P., Ed.; World Scientific Publishing: Singapore, 1995.

(36) Baker, J.; Scheiner, A.; Andzelm, J. *Chem. Phys. Lett.* **1993**, *216*, 380.

(37) Laming, G. J.; Termath, V.; Handy, N. C. *J. Chem. Phys.* **1993**, *99*, 8765.

(38) Pople, J. A.; Gill, P. M.; Handy, N. C. *Int. J. Quantum Chem.* **1995**, *56*, 303.

(39) Foresman, G. J. B.; Keith, T. A.; Wiberg, K. B.; Snoonian J.; Frisch, M. J. *J. Phys. Chem.* **1996**, *100*, 16098.

(40) (a) Laaksonen, L. *J. Mol. Graphics* **1992**, *10*, 33. (b) Bergman, D. L.; Laaksonen, L. *J. Mol. Graphics Modell.* **1997**, *15*, 301.

(41) Weil, J. A.; Bolton, J. R.; Wertz, J. E. *Electron Paramagnetic Resonance*; Wiley and Sons: New York, 1994; pp 240ff.